

SUPPORTING INFORMATION

Factors Influencing the DNA Nuclease Activity of Iron, Cobalt, Nickel, and Copper Chelates

Jeff C. Joyner,^{1,2} Jared Reichfield,¹ and J. A. Cowan^{1,2,3*}

Contribution from ¹ Evans Laboratory of Chemistry, Ohio State University, 100 West 18th Avenue, Columbus, Ohio 43210; ² The Ohio State Biochemistry Program, 784 Biological Sciences 484 W. 12th Avenue, Columbus, Ohio 43210; and ³ MetalloPharm LLC, 1790 Riverstone Drive, Delaware, OH 43015

Correspondence to: Dr. J. A. Cowan, Evans Laboratory of Chemistry, Ohio State University, 100 West 18th Avenue, Columbus, Ohio 43210. tel: 614-292-2703, e-mail: cowan@chemistry.ohio-state.edu

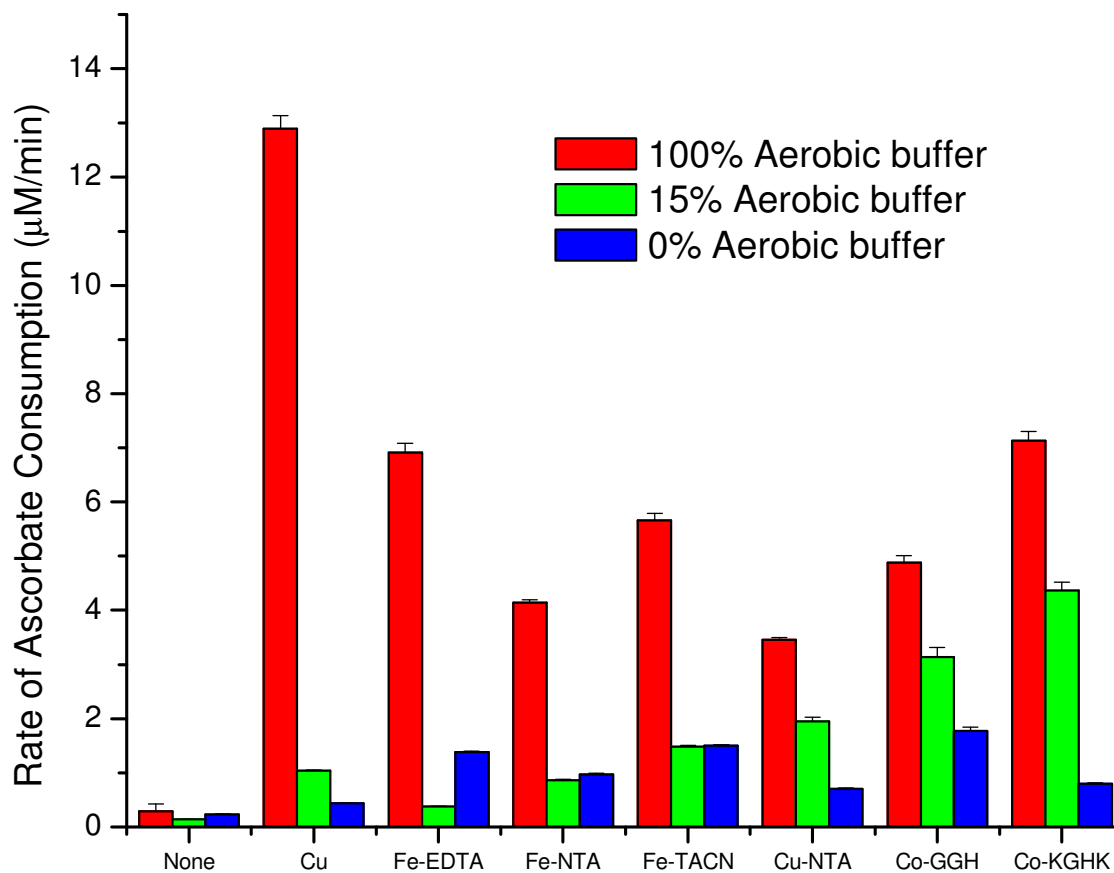


Figure SM1. O₂ requirement for ascorbate consumption for those complexes found to function aerobically in the absence of H₂O₂. Starting reactants included 1 mM ascorbate and 10 μM metal-chelate complex in prepared mixtures of anaerobic (degassed/Ar purged) buffer and aerobic buffer: 100% aerobic (as made), 15% aerobic (by mixing aerobic and anaerobic buffers to a 15:85 ratio within an Ar-purged vial), or ~ 0% aerobic. Rates of ascorbate consumption generally decreased as a higher percentage of purged/degassed buffer was used, consistent with the proposed O₂-dependent mechanisms proposed for these metal complexes.

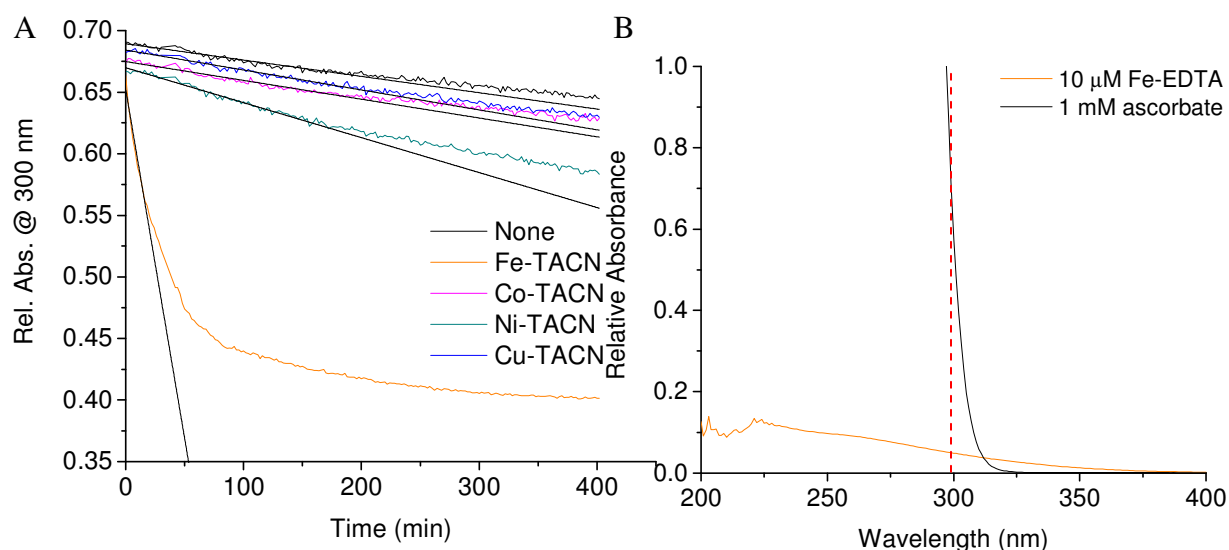


Figure SM2. (A) Sample trace for metal-chelate mediated multiple turnover ascorbate consumption monitored by UV/Vis absorbance. Reactions contained 10 μM Fe(II)-triazacyclononane (or other metal-chelates), 1 mM H_2O_2 , and 1 mM ascorbate in 20 mM HEPES, 100 mM NaCl, pH 7.4 on a clear 96-well plate. Initial rates of ascorbate consumption were determined after monitoring the disappearance of ascorbate at 300 nm. The absorbance from 1 mM ascorbate was ~ 0.68 and from background absorbance was ~ 0.40 . The extinction coefficients for ascorbate and M-chelates at 300 nm are $\sim 590 \text{ M}^{-1}\text{cm}^{-1}$ and $0 - 4,900 \text{ M}^{-1}\text{cm}^{-1}$, respectively (the highest extinction coefficient at 300 nm of $4,900 \text{ M}^{-1}\text{cm}^{-1}$ was observed for Fe-EDTA). Since the concentration of M-chelates used was 100-fold lower than that of ascorbate, the absorbance of 10 μM M-chelate was always less than 10% of the initial absorbance of 1 mM ascorbate. Also, the relatively low absorbance of each M-chelate does not change appreciably during each experiment, especially during steady state turnover, and therefore does not affect the measured slope that occurs as a result of ascorbate consumption. (B) Wavelength scans for 1 mM ascorbate and 10 μM Fe-EDTA, which had the highest extinction coefficient at 300 nm among the M-chelates tested, demonstrating the suitability of the ascorbate and M-chelate concentrations used in the ascorbate consumption assay (300 nm is indicated by the dashed line). Wavelength scans were performed in a quartz cuvette with 1 cm pathlength.

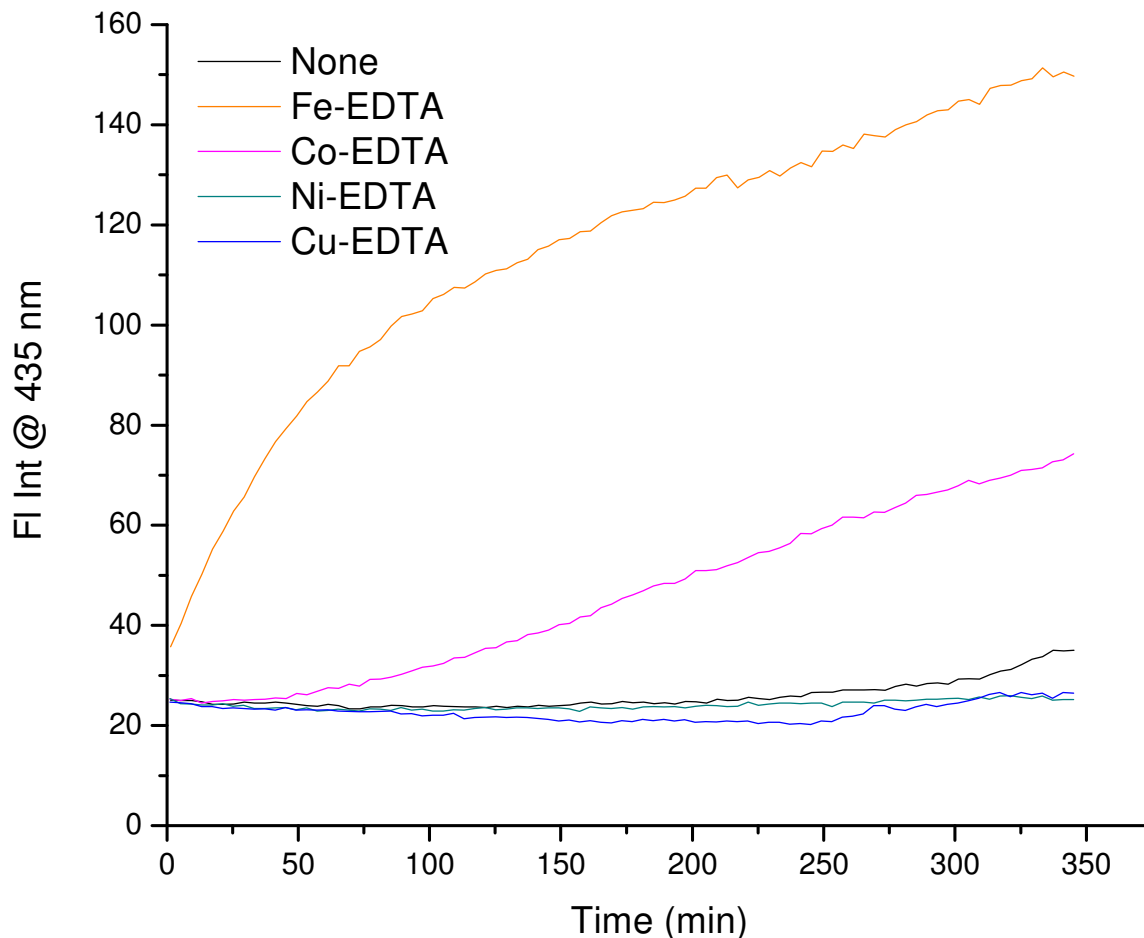


Figure SM3. Sample trace for metal-chelate mediated radical generation monitored by real-time fluorescence of TEMPO-9-AC. Reactions contained 10 μM Fe-EDTA (or other metal-chelates), 10 μM TEMPO-9-AC, and 1 mM H_2O_2 in 20 mM HEPES, 100 mM NaCl, pH 7.4 on a black 96-well plate. Steady-state rates of TEMPO reaction with diffusible radicals were determined after monitoring TEMPO fluorescence at 435 nm. The emission intensity from unreacted TEMPO was ~ 25 units, and for completely reacted TEMPO was ~ 160 units.

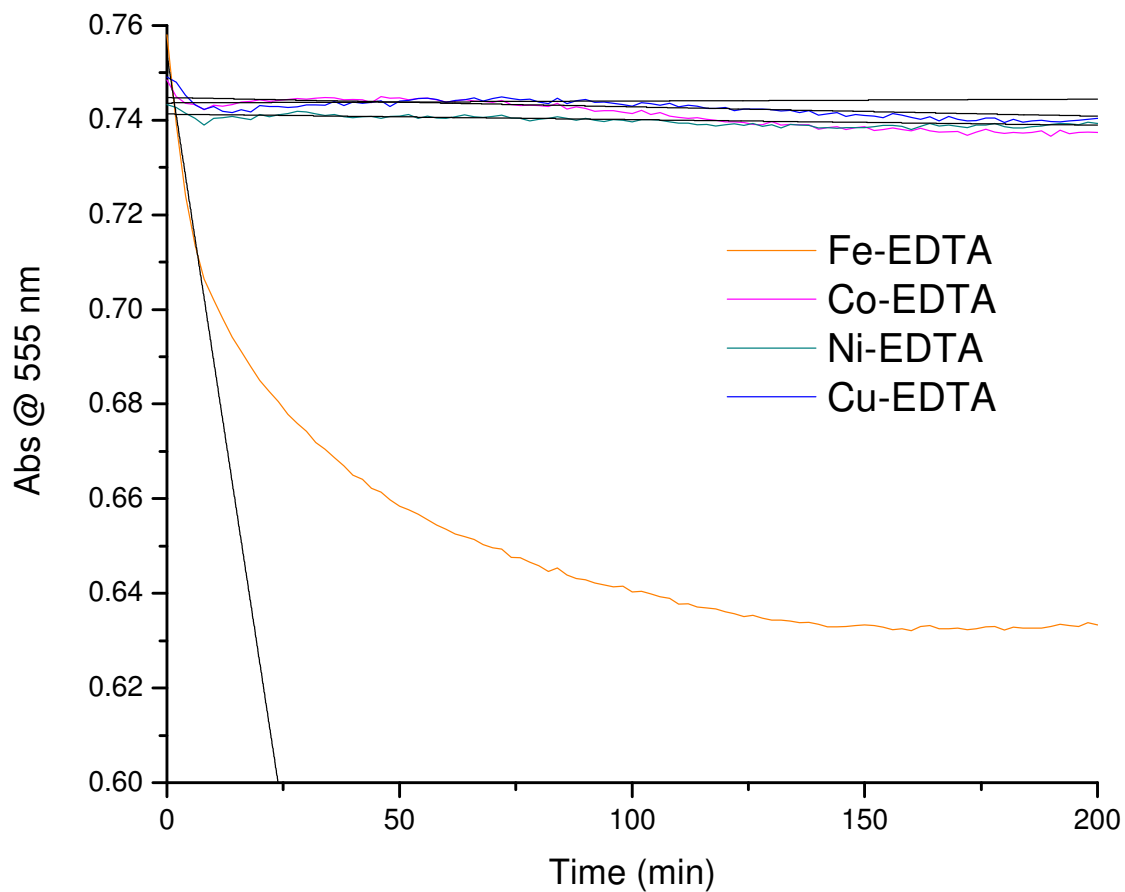


Figure SM4. Sample trace for metal-chelate mediated hydroxyl radical generation monitored by rhodamine B absorbance. Reactions contained 1 μM Fe(II)-EDTA (or other metal-chelates), 10 μM rhodamine B, 1 mM H_2O_2 , and 1 mM ascorbate in 20 mM Na_2HPO_4 , pH 7.4 on a clear 96-well plate. Relative absorbance was monitored at 555 nm and the absorbance from unreacted rhodamine B was ~ 0.74 .

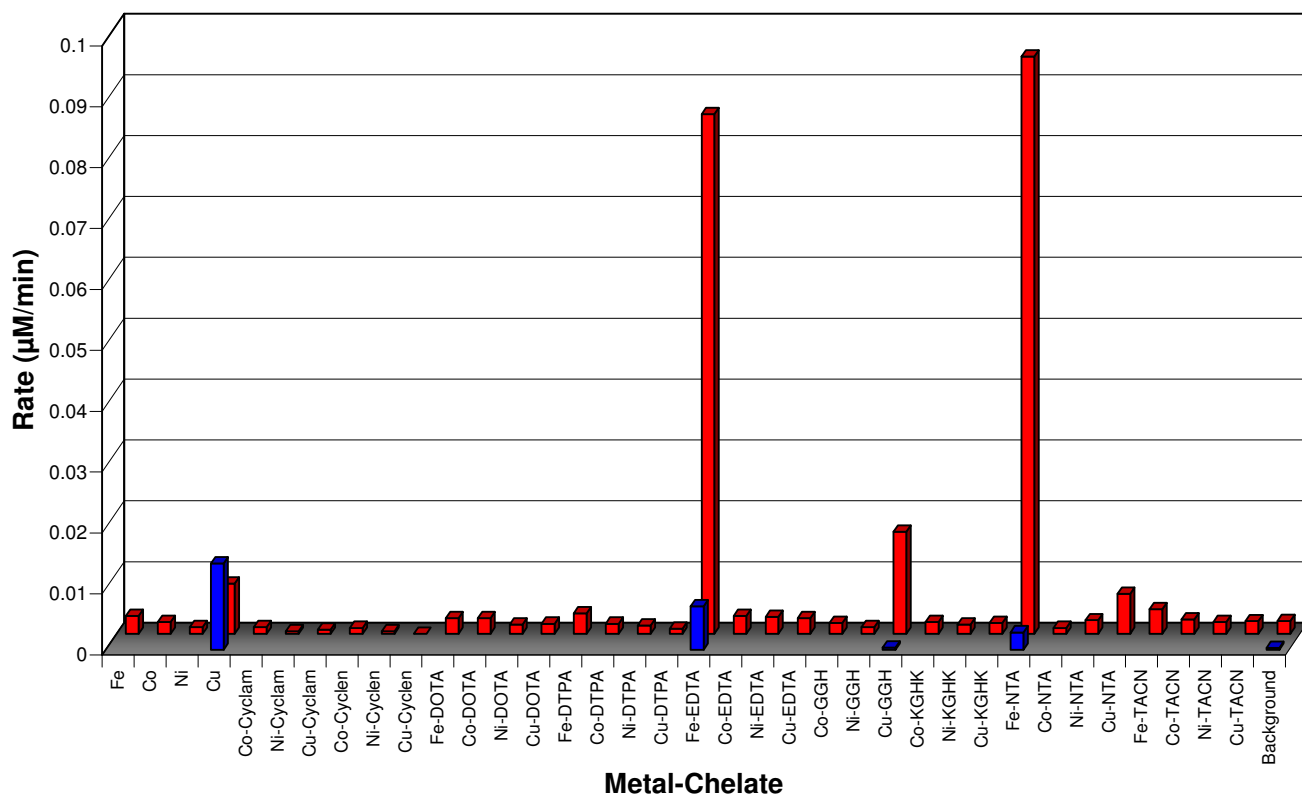


Figure SM5. Summary of initial rates for reaction of rhodamine B with each metal-chelate/O₂ (front) and metal-chelate/H₂O₂ (rear) combination.

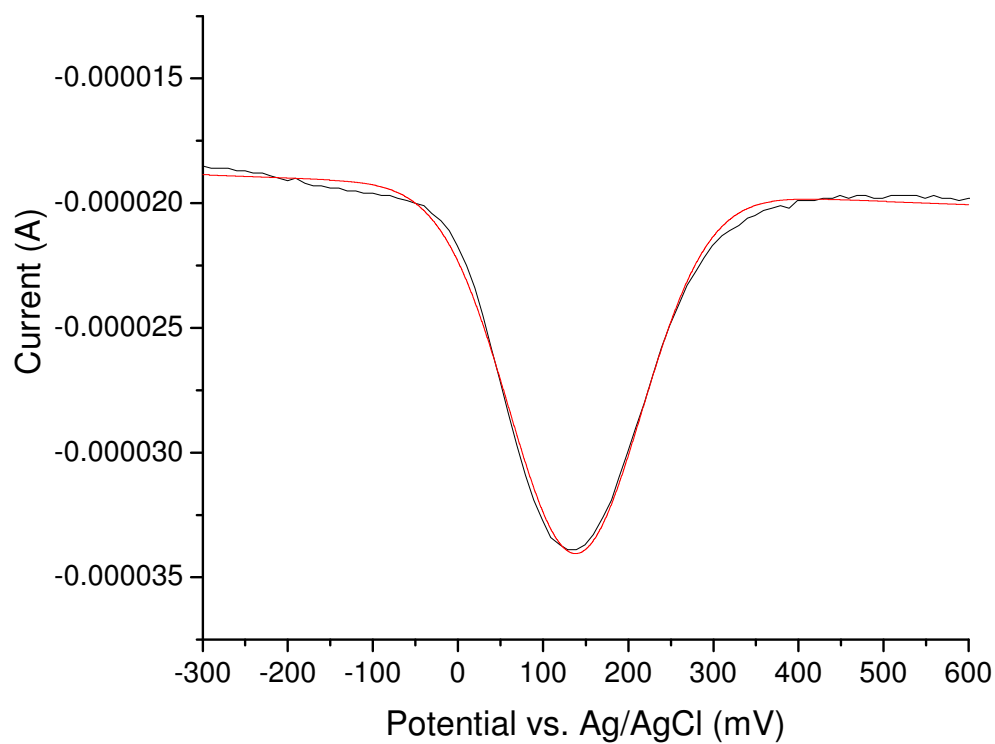


Figure SM6. Representative voltammogram for square wave voltammetry experiments, by which the reduction potentials of metal-chelates (Fe-DOTA shown here) were determined. Each reduction potential was determined by fitting to the Gaussian equation (6) and was later converted from potential vs. Ag/AgCl to vs. NHE. Square wave voltammetry experiments were conducted in an anaerobic solution of 20 mM HEPES, 100 mM NaCl, pH 7.4 at an ambient temperature of ~ 25 °C.

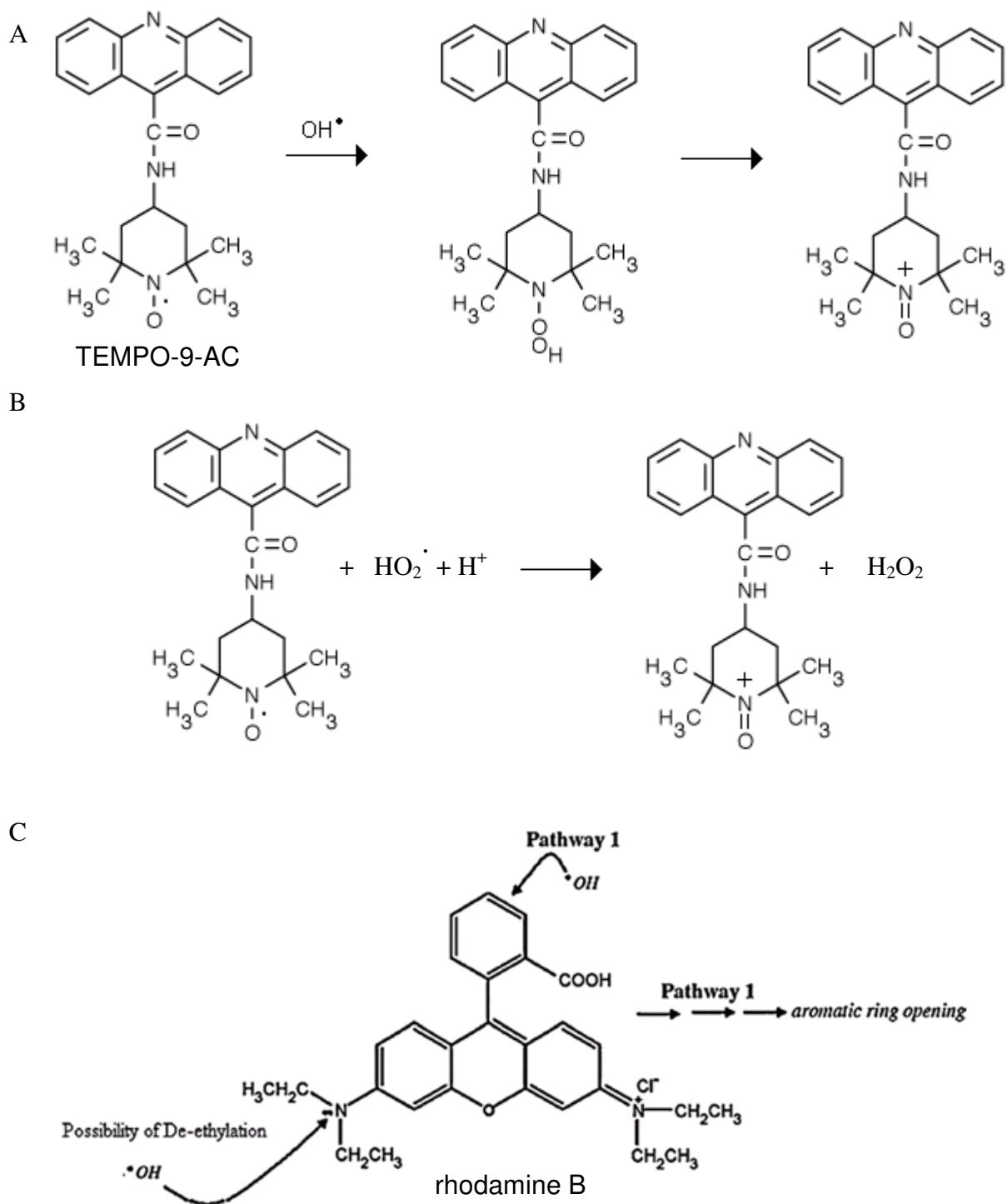


Figure SM7. Structures and pathways for reaction of, (A) TEMPO-9-AC with hydroxyl radical, (B) TEMPO-9-AC with superoxide,^{2,3} and (C) rhodamine B (figure adapted from Mishra et. al. (2010)).⁴ Hydroxyl radical and superoxide radical each react with the nitroxide radical, which quenches the fluorescence of TEMPO-9-AC. Following reaction, the fluorescence of TEMPO is restored.⁵ Limited information is available regarding the mechanism of rhodamine B degradation by hydroxyl radical, although the most likely pathways are aromatic ring opening or de-ethylation.

complex	k_{nick} for DNA nicking (min^{-1})	k_{lin} for DNA linearization (min^{-1})
Fe	0.05 ± 0.01	— ^a
Co	— ^a	0.0009 ± 0.0001
Ni	— ^a	0.0004 ± 0.0001
Cu	0.25 ± 0.05	0.073 ± 0.004
Co-Cyclam	— ^a	— ^a
Ni-Cyclam	— ^a	0.0012 ± 0.0001
Cu-Cyclam	0.053 ± 0.004	0.0008 ± 0.0002
Co-Cyclen	0.017 ± 0.003	— ^a
Ni-Cyclen	— ^a	— ^a
Cu-Cyclen	0.014 ± 0.004	0.0007 ± 0.0001
Fe-DOTA	— ^a	0.0008 ± 0.0001
Co-DOTA	— ^a	0.0005 ± 0.0001
Ni-DOTA	0.030 ± 0.007	0.0029 ± 0.0008
Cu-DOTA	— ^a	0.0013 ± 0.0001
Fe-DTPA	— ^a	0.0012 ± 0.0001
Co-DTPA	— ^a	— ^a
Ni-DTPA	— ^a	— ^a
Cu-DTPA	— ^a	— ^a
Fe-EDTA	0.044 ± 0.009	0.0005 ± 0.0001
Co-EDTA	0.08 ± 0.02	— ^a
Ni-EDTA	0.037 ± 0.002	— ^a
Cu-EDTA	0.032 ± 0.003	— ^a
Co-GGH	— ^a	— ^a
Ni-GGH	— ^a	— ^a
Cu-GGH	0.06 ± 0.01	0.0012 ± 0.0002
Co-KGHK	0.014 ± 0.002	0.0042 ± 0.0008
Ni-KGHK	— ^a	— ^a
Cu-KGHK	0.055 ± 0.008	0.00054 ± 0.00004
Fe-NTA	0.05 ± 0.01	0.0008 ± 0.0002
Co-NTA	0.1 ± 0.1	0.005 ± 0.003
Ni-NTA	— ^a	< 0.009
Cu-NTA	0.148 ± 0.007	0.0032 ± 0.0004
Fe-TACN	0.012 ± 0.006	0.0008 ± 0.0007
Co-TACN	— ^a	— ^a
Ni-TACN	— ^a	— ^a
Cu-TACN	— ^a	— ^a
Background	0.006 ± 0.001	0.00024 ± 0.00003

Table SM1. Summary of observed first-order rate constants (k_{obs}) for consecutive DNA nicking (k_{nick} , rear) and subsequent linearization (k_{lin} , front) by each metal-chelate (as shown in Figure 1 of the manuscript). ^a Below detection limit. The limits of detection for nicking and linearization were 0.009 and 0.00033 min^{-1} , respectively.

complex	k_{nick} for DNA nicking (min^{-1})	ascorbate consumption rate for H_2O_2 and $\{\text{O}_2\}$ ($\mu\text{M}/\text{min}$)	TEMPO reaction rate for H_2O_2 and $\{\text{O}_2\}$ ($\mu\text{M}/\text{min}$)	reduction potential vs. NHE (mV)	redox couple
Fe	0.05 ± 0.01	6.4 ± 0.1 {--- ^a }	--- ^a {--- ^a }	-- ^b	3+/2+
Co	--- ^a	--- ^a {--- ^a }	0.0319 ± 0.0009 {--- ^a }	-- ^b	3+/2+
Ni	--- ^a	--- ^a {--- ^a }	0.0156 ± 0.0003 {--- ^a }	-- ^b	2+/1+
Cu	0.25 ± 0.05	80 ± 10 { 12.9 ± 0.2 }	0.16 ± 0.01 {--- ^a }	136 ¹	2+/1+
Co-Cyclam	--- ^a	--- ^a {--- ^a }	0.0175 ± 0.0002 {--- ^a }	61 ^c	3+/2+
Ni-Cyclam	--- ^a	--- ^a {--- ^a }	--- ^a {--- ^a }	-275 ^c	2+/1+
Cu-Cyclam	0.053 ± 0.004	--- ^a {--- ^a }	--- ^a {--- ^a }	163 ^c	2+/1+
Co-Cyclen	0.017 ± 0.003	--- ^a {--- ^a }	--- ^a { 0.0124 ± 0.0002 }	-228 ^c	3+/2+
Ni-Cyclen	--- ^a	--- ^a {--- ^a }	--- ^a {--- ^a }	-211 ^c	2+/1+
Cu-Cyclen	0.014 ± 0.004	--- ^a {--- ^a }	--- ^a {--- ^a }	280 ^c	2+/1+
Fe-DOTA	--- ^a	--- ^a {--- ^a }	0.0601 ± 0.0005 {--- ^a }	396 ¹	3+/2+
Co-DOTA	--- ^a	--- ^a {--- ^a }	--- ^a {--- ^a }	142 ¹	3+/2+
Ni-DOTA	0.030 ± 0.007	--- ^a {--- ^a }	--- ^a {--- ^a }	-35 ¹	2+/1+
Cu-DOTA	--- ^a	--- ^a {--- ^a }	--- ^a {--- ^a }	180 ¹	2+/1+
Fe-DTPA	--- ^a	--- ^a {--- ^a }	0.0185 ± 0.0005 {--- ^a }	280 ¹	3+/2+
Co-DTPA	--- ^a	--- ^a {--- ^a }	--- ^a {--- ^a }	1111 ¹	3+/2+
Ni-DTPA	--- ^a	--- ^a {--- ^a }	--- ^a {--- ^a }	-- ^b	2+/1+
Cu-DTPA	--- ^a	--- ^a {--- ^a }	--- ^a {--- ^a }	148 ¹	2+/1+
Fe-EDTA	0.044 ± 0.009	80 ± 10 { 6.9 ± 0.2 }	0.078 ± 0.001 { 0.0222 ± 0.0006 }	391 ¹	3+/2+
Co-EDTA	0.08 ± 0.02	--- ^a {--- ^a }	0.0185 ± 0.0003 {--- ^a }	146 ¹	3+/2+
Ni-EDTA	0.037 ± 0.002	--- ^a {--- ^a }	--- ^a {--- ^a }	172 ¹	2+/1+
Cu-EDTA	0.032 ± 0.003	--- ^a {--- ^a }	--- ^a {--- ^a }	47 ¹	2+/1+
Co-GGH	--- ^a	0.5 ± 0.2 { 4.9 ± 0.1 }	--- ^a {--- ^a }	-119 ¹	3+/2+
Ni-GGH	--- ^a	--- ^a {--- ^a }	--- ^a {--- ^a }	1000 ¹	3+/2+
Cu-GGH	0.06 ± 0.01	2.72 ± 0.08 {--- ^a }	--- ^a {--- ^a }	1038 ¹	3+/2+
Co-KGHK	0.014 ± 0.002	0.5 ± 0.2 { 7.1 ± 0.2 }	--- ^a {--- ^a }	-228 ¹	3+/2+
Ni-KGHK	--- ^a	--- ^a {--- ^a }	--- ^a {--- ^a }	1055 ¹	3+/2+
Cu-KGHK	0.055 ± 0.008	--- ^a {--- ^a }	--- ^a {--- ^a }	1058 ¹	3+/2+
Fe-NTA	0.05 ± 0.01	130 ± 20 { 4.15 ± 0.04 }	0.145 ± 0.002 { 0.0449 ± 0.0005 }	464 ¹	3+/2+
Co-NTA	0.1 ± 0.1	--- ^a {--- ^a }	0.075 ± 0.002 {--- ^a }	274 ¹	3+/2+
Ni-NTA	--- ^a	--- ^a {--- ^a }	--- ^a {--- ^a }	176 ¹	2+/1+
Cu-NTA	0.148 ± 0.007	0.72 ± 0.05 { 3.46 ± 0.04 }	--- ^a {--- ^a }	215 ¹	2+/1+
Fe-TACN	0.012 ± 0.006	17 ± 1 { 5.7 ± 0.1 }	25.94 ± 0.02 { 0.0099 ± 0.0001 }	175 ^c	3+/2+
Co-TACN	--- ^a	--- ^a {--- ^a }	--- ^a {--- ^a }	-362 ^c	3+/2+
Ni-TACN	--- ^a	--- ^a {--- ^a }	--- ^a {--- ^a }	991 ^c	2+/1+
Cu-TACN	--- ^a	--- ^a {--- ^a }	--- ^a {--- ^a }	110 ^c	2+/1+
Background	0.006 ± 0.001	0.6 ± 0.6 { 0.3 ± 0.1 }	0.007 ± 0.003 { 0.0039 ± 0.0007 }		

Table SM2. Summary of observed rate constants for DNA nicking reactions (k_{nick}) promoted by M-chelates/ H_2O_2 /ascorbate, arranged by chelating ligand. Initial rates for ascorbate consumption (with and without H_2O_2 as an added coreactant) and radical generation (again, with and without added H_2O_2), as well as the reduction potential for each M-chelate, are listed for comparison. Redox couples are 3+/2+ for Fe, Co, Ni-ATCUN, and Cu-ATCUN complexes and 2+/1+ for all other Ni and Cu complexes. ^a Below detection limit. ^b Not determined. ^c This work.

SM References

- (1) Joyner, J. C.; Cowan, J. A. *J. Am. Chem. Soc.* **2011**, *133*, 9912–9922.
- (2) Samuni, A.; Goldstein, S.; Russo, A.; Mitchell, J. B.; Krishna, M. C.; Neta, P. *J. Am. Chem. Soc.* **2002**, *124*, 8719-8724.
- (3) Bar-On, P.; Mohsen, M.; Zhang, R.; Feigin, E.; Chevion, M.; Samuni, A. *J. Am. Chem. Soc.* **1999**, *121*, 8070-8073.
- (4) Mishra, K. P.; Gogate, P. R. *Separ. Purif. Technol.* **2010**, *75*, 385-391.
- (5) Laight, D. W.; Andrews, T. J.; Haj-Yehia, A. I.; Carrier, M. J.; Änggård, E. E. *Env. Tox. Pharm.* **1997**, *3*, 65-68.

Complete Reference 8 from Manuscript

Hacein-Bey-Abina, S.; Kalle, C. V. S., M.; M.P., M.; Wulffraat, N.; Leboulch, P.; Lim, A.; Osborne, C. S.; Pawliuk, R.; Morillon, E.; Sorenson, R.; Forster, A.; Fraser, P.; Cohen, J. I.; de Saint Basile, G.; Alexander, I.; Wintergest, U.; Frebourg, T.; Aurias, A.; Stoppa-Lyonnet, D.; Romana, S.; Radford-Weiss, I.; Gross, F.; Valensi, F.; Delabesse, E.; Macintyre, E.; Sigaux, F.; Soulier, J.; Leiva, L. E.; Wissler, M.; Prinz, C.; Rabbitts, T. H.; Le Deist, F.; Fischer, A.; Cavazzana-Calvo, M. *Science* **2003**, *302*, 415.